

Article

Influence of Copper-Based Fillers on Structural and Mechanical Properties of Polylactic Acid Composites

Elena Evgenyevna Mastalygina ^{1,2,*} , Anatoly Aleksandrovich Olkhov ^{1,2,3} ,
Nikolay Vladimirovich Vorontsov ^{1,2}, Nikolay Vitalievich Kiselev ^{1,2,4,*} , Timur Bakhtierovich Khaidarov ^{1,4},
Bekzod Bakhtierovich Khaydarov ⁴ , Evgeniy Aleksandrovich Kolesnikov ⁴
and Igor Nikolaevich Burmistrov ^{1,2,4} 

- ¹ Higher School of Engineering, Plekhanov Russian University of Economics, 36 Stremyanny Ln, Moscow 117997, Russia
² Institute of Biochemical Physics Named after N.M. Emanuel, Russian Academy of Sciences, 4 Kosygin St, Moscow 119991, Russia
³ N.N. Semenov Federal Research Center for Chemical Physics, Russian Academy of Sciences, 4 Kosygin St, Moscow 119334, Russia
⁴ Department of Functional Nanosystems and High-Temperature Materials, National University of Science & Technology «MISIS», 4 Leninsky Pr, Moscow 119049, Russia
* Correspondence: elena.mastalygina@gmail.com or mastalygina.ee@rea.ru (E.E.M.); nikokisely12345@gmail.com (N.V.K.)



Citation: Mastalygina, E.E.; Olkhov, A.A.; Vorontsov, N.V.; Kiselev, N.V.; Khaidarov, T.B.; Khaydarov, B.B.; Kolesnikov, E.A.; Burmistrov, I.N. Influence of Copper-Based Fillers on Structural and Mechanical Properties of Polylactic Acid Composites. *J. Compos. Sci.* **2022**, *6*, 386. <https://doi.org/10.3390/jcs6120386>

Academic Editor: Ahmed Koubaa

Received: 28 October 2022

Accepted: 8 December 2022

Published: 13 December 2022

Publisher's Note: MDPI stays neutral with regard to jurisdictional claims in published maps and institutional affiliations.



Copyright: © 2022 by the authors. Licensee MDPI, Basel, Switzerland. This article is an open access article distributed under the terms and conditions of the Creative Commons Attribution (CC BY) license (<https://creativecommons.org/licenses/by/4.0/>).

Abstract: The importance of promising composites in modern materials science is constantly increasing. The use of various fillers or additives is associated with their influence not only on the defining properties of the composite, but also on physical and mechanical characteristics of the material. In this case, the distribution of the additive and its wetting with a polymer play an important role. The problem highlighted in this article is the influence of different copper-containing fillers (copper (II) sulphate powder, micro-sized copper (II) oxide powder, and nano-structured copper (II) oxide-based hollow microspheres) on the technological and physical–mechanical properties of the composites based on polylactic acid (PLA). The hollow microspheres of copper (II) oxide have been obtained by ultrasonic spray atomization via pyrolysis of copper (II) nitrate. The structure of the copper-based additives has been studied using X-ray diffraction, scanning electron microscopy, and static light scattering. For the PLA-composites, scanning electron microscopy, differential scanning calorimetry, stress-strain properties testing, and density analysis have been performed. The plasticizing effect of polycaprolactone and polyethylene glycol has been studied for the highly filled PLA/CuSO₄ composite. The samples of PLA with over 2 wt.% of CuO microspheres have a full volume-filling and percolation structure of the additive's particles. Due to the regular spherical shape of the particles and a lower specific volume, CuO hollow microspheres are uniformly distributed in the PLA matrix acting as a structuring and reinforcing modifier. Differential scanning analysis showed heterogeneous crystallization on CuO particles with an increase in the degree of crystallinity and the melting point of the polymer. It has been shown that the pre-masterbatching technology and adding plasticizers to obtain PLA composites contribute minimizing defects and enhance mechanical properties.

Keywords: polylactic acid; polylactide; antimicrobial properties; copper (II) sulphate; copper (II) oxide; hollow microspheres; reinforcing additive; heterogeneous crystallization

1. Introduction

The development of biodegradable polymeric materials with additional features is one of the current scientific directions. Since polymers are widely used in medical products, including those that contact human cells, as well as food packaging products, researchers are increasingly seeking to impart antimicrobial activity to such materials.

The main difficulties in creating such antimicrobial materials are to give a certain level of antimicrobial activity while maintaining high physical and mechanical properties of the materials, to develop an antimicrobial additive with high thermal stability to enable processing of molten polymeric materials, and to minimize the negative effects of an active additive on biodegradation of the product after its life cycle.

Various methods of giving antimicrobial properties to polymeric materials are known, particularly blending with active additives or coating by them. At the same time, additives of various chemical natures are used: from commercial antibiotics to metal compounds of different dispersion. The materials based on polypropylene [1], polylactic acid [2], polyester [3], and polyurethane [4] containing the thermostable antibiotic ciprofloxacin are known. In addition, commercial antibiotics such as vancomycin [5], ceftriaxone [6], and cefpodoxime [7] are used to impart antimicrobial properties to polymers. Bacterio- and fungicidal products based on polyphenols [8,9] and polyphosphonates [10] are also actively used.

Different metal compounds, for example, silver, copper, zinc, iron, and manganese, also have high antibacterial, antiviral, and antifungal properties. The antibacterial activity of metals is based on the production of reactive oxygen species and free radicals, protein dysfunction and loss of enzyme activity, damaging cell membranes and disruption of electron transport, and impairment of nutrient absorption [11]. Metals are used directly, as well as metal-containing additives for polymer materials [12,13], metal oxides and salts [14–16], and metal complexes [17].

Dispersed additives can significantly affect mechanical properties of polymers, both reducing [18,19] and improving [20] them. To ensure good distribution of a metal-containing additive in the polymer matrix and to level the negative effect of an additive on the technological and physical–mechanical properties of materials, various polymer modification technologies are used. Works devoted to surface treatment with antimicrobial agents [12,21], addition of particles through the polymer solution [6,22], the use of nano-sized additive particles [23], and others are known.

An ability of copper and its compounds to slow down or even inhibit the growth of pathogenic microorganisms has been proven in numerous works. Copper has sufficient biocidal activity (about 10 mg Cu^{2+} per kg of water is required to kill 10^6 cells of *Saccharomyces cerevisiae*) [24]. However, copper ions can be easily mobilized by oxidation, so typically copper compounds are used to modify polymers [16,25–27].

According to the previous studies, the functional activity of copper correlates with its concentration, including the rate of ion release [12]. In this regard, researchers use copper in different forms, for instance in the form of salts or oxides with different sizes and shapes of additive particles. In the present study, we used finely ground powder of copper (II) sulphate, powder of copper (II) oxide, and specially synthesized hollow copper (II) oxide microspheres. Various methods of producing hollow particles or microspheres [28,29] are used to save the consumption of active additive. Reduced density of particles is also preferred for uniform distribution in the solution or melt of polymer [30].

Such copper particles are currently only obtained using various physicochemical methods. In [31], micro-sized hollow spherical copper and copper oxide particles were produced by the reduction of copper 2-[2-(2-methoxyethoxy)ethoxy]acetate with benzyl alcohol at 195 °C. Another study [32] focused on a synthesis of hollow Cu_2O microspheres by forming low density aggregates in aqueous solution with polyvinylpyrrolidone followed by transformation into hollow spheres by Ostwald ripening. Monodispersed Cu_2O was synthesized by a simple polyol reduction method using various copper salts [33].

The influence of copper-based antimicrobial additives on the technological and mechanical properties of polylactides has not been studied in depth. For this reason, the main goal of the presented paper is the investigation of the different copper-based fillers effects on the technological and physical–mechanical properties of the PLA composite. At the same time, the study of the influence of previously unexplored fillers based on hollow

microspheres of copper oxide synthesized by the spray pyrolysis method is studied in the paper.

2. Materials

The objects of study were sheet materials based on polylactic acid (polylactide) (hereinafter, PLA) with copper-based antibacterial additives. Polylactide was chosen as a matrix as the most widespread and cheap polymer from polyesters characterized by high ability to enzymatic hydrolysis, biocompatibility, and inertia [34]. PLA (Ingeo 4043D, Nature Works, LLC, Plymouth, MI, USA) with an MFI of 6 g/10 min (210 °C, 2.16 kg) and a density of 1.24 g/cm³ was used. Plasticizing additives were used to enhance the homogeneous distribution of particles of antibacterial additives and increase elasticity of the composites' samples. Polycaprolactone (600C, Shenzhen ESUN Industrial Co., Ltd., Shenzhen, China) (hereinafter, PCL) and polyethylene glycol (PEG-400, NorPeg 400, LLC "Norkem") (hereinafter, PEG) were used as plasticizers.

The following antibacterial additives were used:

1. Copper (II) sulphate (CuSO₄) powder (Component-Reagent LLC, Moscow, Russia);
2. Copper (II) oxide (CuO) powder (Nanostructured and Amorphous Materials, Inc., Houston, TX, USA);
3. Hollow copper (II) oxide microspheres (CuO shp) synthesized by the authors, not previously studied as antibacterial additives for polymers.

The characterization of the applied commercial raw materials according to the technical documentation is given in Table 1.

Table 1. Characterization of raw materials for the composites.

Name Parameter	Polylactic Acid (Poly-Lactide)	Polycapro- Lactone	Polyethylene Glycol	Copper (II) Sulfate Penta-Hydrate Powder	Copper (II) Oxide Powder
Abbreviation	PLA	PCL	PEG	CuSO ₄	CuO
Trade mark, producer	Ingeo 4043D, Nature Works, LLC (USA)	600C, Shen- zhen ESUN Industrial Co., Ltd (China)	NorPeg 400, LLC "Norkem"	Component-Reagent LLC, Moscow, Russia	Nanostructured and Amorphous Materials, Inc., Houston, TX, USA
Description	thermoplastic aliphatic polyester	thermoplastic aliphatic polyester	low-molecular- weight grade of polyethy- lene glycol	CuSO ₄ × 5H ₂ O, GOST 4165-78; purity: 98%	purity: 99%
Molecular weight (g/mol)	155,000–165,000	50,000–60,000	380–440	249.69	79.55
Melt flow index (g/10 min)	5–7 (210 °C, 2.16 kg)	11–12 (160 °C, 2.16 kg)	-	-	-
Density (g/cm ³)	1.21–1.25	1.08–1.12	1.1–1.2	2.3–3.6	6.1–6.6
Melting point (°C)	145–160	58–60	4–8	-	-

Hollow copper (II) oxide microspheres were synthesized by an ultrasonic spray pyrolysis method developed by the authors. The synthesis unit consists of a glass vessel, high-frequency ultrasonic generators, a tubular furnace, a quartz reactor, a filter for collecting samples, and pumps (Figure 1). This method of particle synthesis makes it possible to obtain hollow microspheres with a diameter of 0.5 to 10 µm, which consist of nanosized particles less than 30 nm. Previously, the authors have successfully synthesized similar hollow microspheres based on nickel oxide [35].

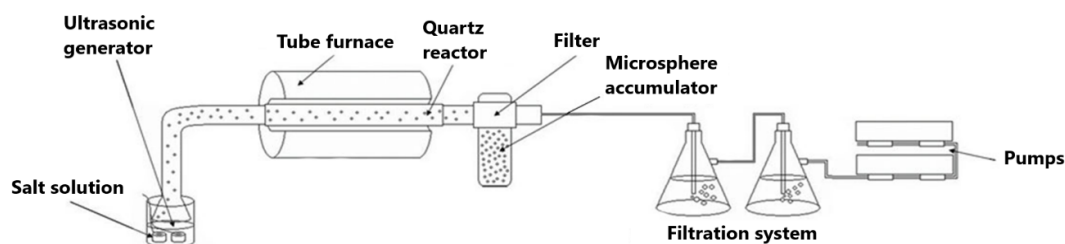


Figure 1. Scheme of synthesis of hollow copper (II) oxide microspheres.

The principle of microsphere production was in pyrolysis of copper (II) nitrate solution in the form of an aerosol in a high-temperature reactor. High-frequency ultrasonic generators with a frequency of 22.4 kHz were immersed in a vessel with a 10 wt.% solution of copper (II) nitrate. The ultrasonic treatment produced a dispersed aerosol of copper (II) nitrate solution. The amount of solution was kept constant to produce microspheres with a minimum size distribution. The aerosol generated by ultrasonic generators was drawn into the furnace reactor at a rate of 16 liters per minute through nozzles by air pumps. Filtered air was used as a carrier gas. The temperature inside the reactor was 1000 °C. Under the high temperature, on the surface of the drop of salt solution a salt layer was formed and then decomposed with the formation of oxide. A schematic representation illustrating the principle of hollow copper (II) oxide microspheres formation is shown in Figure 2. From the reactor, the heated mixture passed through a filter that separated the obtained oxide particles from the gas stream. The gases formed during pyrolysis were removed further. To neutralize aggressive gases, a system of flasks partially filled with water was used. Aggressive gases passing through the filtration system with water flasks formed diluted acid. The remaining gas mixture was then pumped out.

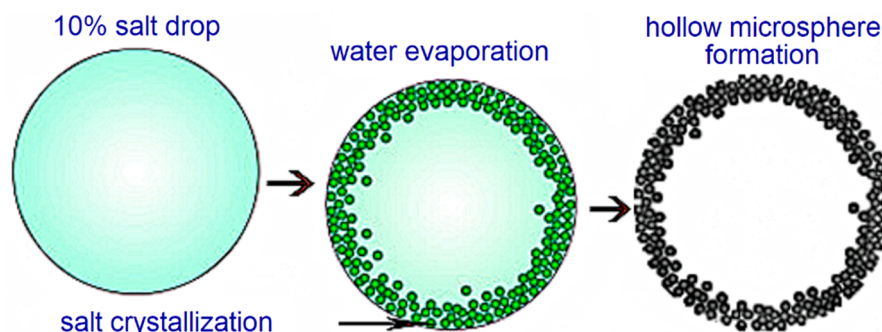


Figure 2. Formation scheme of hollow copper (II) oxide microspheres.

The studied antimicrobial additives were introduced into the PLA-matrix using pre-masterbatching technology, i.e., prefabrication of highly filled superconcentrates. The efficiency of pre-masterbatching has been shown by P.G. Shelenkov, et al. [36].

All the components were pre-conditioned in a heat chamber for 1 h at temperatures from 60 to 100 °C, depending on the melting temperatures of the components. Next, the appending of additive particles to the polymer matrix was made by the pre-processing superconcentrates using the solution technology. A portion of pelletized PLA was dissolved in dichloromethane (methylene chloride) at a concentration of 8 g/100 mL using a magnetic stirrer at 400–500 rpm and 30–35 °C for 1 h. Then, an antibacterial additive was added to the PLA solution at a ratio of PLA/additive = 50/50 wt.% and mixed for 1 h. After that, the composite sheets were formed by pouring the suspension onto glass Petri dishes. The moulded sheets were dried at room temperature for 24 h until the solvent completely evaporated. After removing the sheets of material from the Petri dishes, they were milled to fragments with a size of 1–3 mm. Then, the obtained superconcentrates of 50 PLA/50 additive (wt.%) was mixed with matrix PLA.

The final composites of PLA with various antimicrobial additives were obtained using heated mixing rollers BL-6175-BL (Dongguan BaoPin International Precision Instruments Co., Ltd., Dongguan, China) at a roller speed of 10 rpm and a temperature of $(190 \pm 5)^\circ\text{C}$ for 10 min. Plasticizing additives (PCL and PEG) were added directly to the PLA melt during the process of mixing a superconcentrate with a matrix polymer.

Then, the materials were pelletized and sheets were pressed in aluminium moulds with polyimide substrates using a laboratory hydraulic press RPA-12 (Biolent, Russia) at a temperature of $(190 \pm 5)^\circ\text{C}$ and a pressure of 50 kgf/cm^2 with subsequent quenching in water at $(20 \pm 2)^\circ\text{C}$. As a result, sheet materials with thickness of $0.7 \pm 0.1\text{ mm}$ were obtained. The compositions of all the obtained samples are shown in Table 2.

Table 2. Compositions of PLA-based materials with various modifiers.

Sample Name	PLA, wt. %	Plasticizer, wt. %	Antimicrobial Additive, wt. %
PLA (neat)	100.0	-	-
PEG + 5 CuSO ₄	90.0	PEG, 5.0	CuSO ₄ , 5.0
PEG + 10 CuSO ₄	85.0	PEG, 5.0	CuSO ₄ , 10.0
PEG + PCL + 10 CuSO ₄	75.0	PEG, 5.0; PCL, 10.0	CuSO ₄ , 10.0
0.5 CuO	99.5	-	CuO, 0.5
1 CuO	99.0	-	CuO, 1.0
2 CuO	98.0	-	CuO, 2.0
5 CuO	95.0	-	CuO, 5.0
0.5 CuO sph	99.5	-	CuO sph, 0.5
1 CuO sph	99.0	-	CuO sph, 1.0
2 CuO sph	98.0	-	CuO sph, 2.0
5 CuO sph	95.0	-	CuO sph, 5.0

3. Methods

3.1. Determination of Chemical Structure and Dimensional Parameters of Particles of Antimicrobial Additives

To determine chemical composition and purity of the synthesized particles X-ray diffraction (XRD) method was used. X-ray diffractograms were obtained at $(25 \pm 1)^\circ\text{C}$ on a Difrax-401k X-ray diffractometer with a position-sensitive gas-filled detector (Scientific Instruments, Moscow, Russia) with a 100 W tube (Cr-K α radiation, $\lambda = 0.229\text{ nm}$). The operating voltage and current were 25 kV and 4 mA, respectively. Data were collected from 15 to $140^\circ 2\theta$ with an interval of $0.02^\circ 2\theta$.

The density was determined by helium pycnometry (Pycnomatic ATC, Thermo Scientific, Waltham, MA, USA) at $(25 \pm 2)^\circ\text{C}$. Particle size parameters were analyzed in aqueous suspensions at $(25 \pm 1)^\circ\text{C}$ using a laser particle size analyzer (Bettersiser ST, Liaoning, China). Pre-mixing was carried out using an overhead stirrer at 1600 rpm and simultaneous exposure to a 5 W ultrasonic dispersant for 2 min. Then, measurements were made using the Mi optical mode (considering the refractive index of the substance). Due to a high solubility of copper (II) sulphate in water, its dimensional parameters (Feret diameter) were analyzed using an optical microscope Axio Lab.A1 (Zeiss, Jena, Germany) and the ImageJ particle parameter analysis program.

3.2. Scanning Electron Microscopy (SEM)

The morphology of the antimicrobial additives' particles and the obtained polymeric materials was investigated using a scanning electron microscope Tescan Vega 3 (TESCAN ORSAY HOLDING, a.s., Brno-Kohoutovice, Czech Republic) with a thermo-emission tungsten cathode. The results were processed using the Tescan Vega 3 control software (ver. 4.2.30.0, Tescan, Brno, Czech Republic). The chipped samples of the polymer composites obtained after keeping the materials in liquid nitrogen for 20 min were analyzed. Conductive magnetron sputtering of platinum coating with a thickness of 20 nm were made using

the Jeol JFC-1600 (Tokyo, Japan). Accelerating voltage was 20 kV with a working distance of 10–15 mm.

3.3. Differential Scanning Calorimetry (DSC)

The processes of glass transition, cold crystallization, and melting of PLA were studied by a differential scanning calorimeter DSC 214 Polyma (NETZSCH-Geratebau GmbH, Selb, Germany) according to ISO 11357-3:2018. The heating of the samples was carried out in the temperature range of 20–200 °C at a scanning speed of 10 °C/min. The samples' weight was 8 ± 0.5 mg. A temperature scale and an enthalpy of melting were calibrated against indium, zinc, and stannic standard samples.

3.4. Tensile Strength Properties

Determining tensile strength properties of the samples was made using a Devotrans DVT GP UG 5 testing machine (Turkey) in accordance with BS EN ISO 527-1 and BS EN ISO 527-3 standards. The samples were cut out on a pneumatic punching press GT-7016-AR (GOTECH testing Machines, Inc., Taichung City, Taiwan) according to BS EN ISO 527-3:1996 (type 1B). Tests were carried out at a tensile speed of 10 mm/min, a working length of 60 mm, and a number of repetitions for each type of material of at least 5. The ultimate tensile strength (σ_{max}), relative elongation at break (ϵ_b), and elastic modulus in the elastic strain region (E) were calculated from the obtained tensile diagrams.

3.5. Hydrostatic Weighing

Measurement of the samples' density was performed by the hydrostatic weighing method with an analytical balance AND GR-200 (Japan) and a density determination kit (AD-1654 HR-AZ). A sample with a size of 10 × 10 cm was weighed in air then weighed when immersed in bidistilled water at (24 ± 0.5) °C. The sample's density was calculated using Formula (1):

$$\rho = \frac{m_{air}}{|m_{air} - m_{water}|} \times \rho_0 \quad (1)$$

where ρ —density of sample (g/cm^3), m_{air} —weight of sample in air (g), m_{water} —weight of sample in water (g), and $\rho_0 = 0.9973 \text{ g}/\text{cm}^3$ —density of water at 24 °C (according to the reference table).

4. Results and Discussion

4.1. Characterization of Antimicrobial Additives

According to the obtained X-ray diffractogram of the microspheres' sample based on copper oxide, the presence of a phase corresponding to the chemical composition of copper (II) oxide CuO was found (Figure 3). In addition, a significant widening of the maxima was observed, which could indicate a small size of the coherent scattering regions.

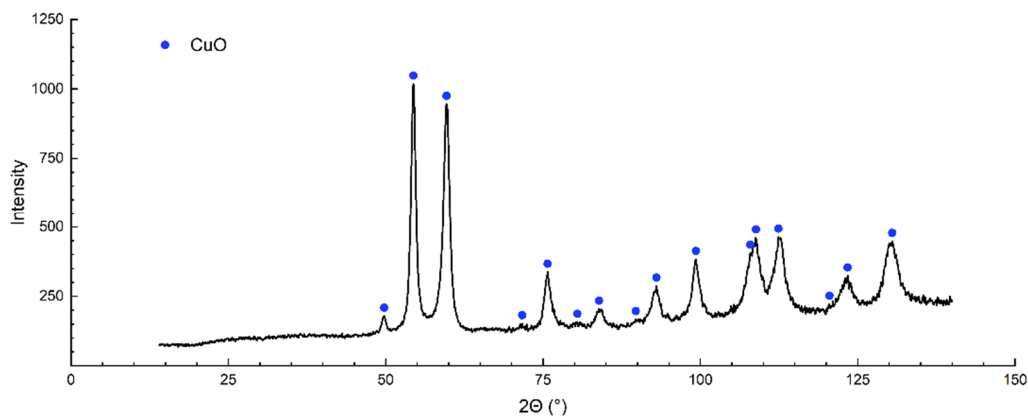


Figure 3. X-ray diffraction pattern of copper (II) oxide microspheres (CuO sph).

The results of the analysis of particle size parameters of antimicrobial additives are shown in Figure 4. The size of copper sulphate particles was not studied by DLS method due to its solubility in water. According to optical microscopy data, the average particle size ranges from 1 to 4 μm (Figure 4a). It is important to note that it is quite easy to crush and can be additionally dispersed when added to the melted polymer. The particles of the commercial CuO powder were characterized by a particle size ranging from 10 to 100 μm (Figure 4b) with a predominant fraction of particles between 20–75 μm (74.4%). The particle size range of CuO microspheres was 0.5–20 μm with the largest fraction of particles between 1 and 5 μm in size (66.5%) (Figure 4c).

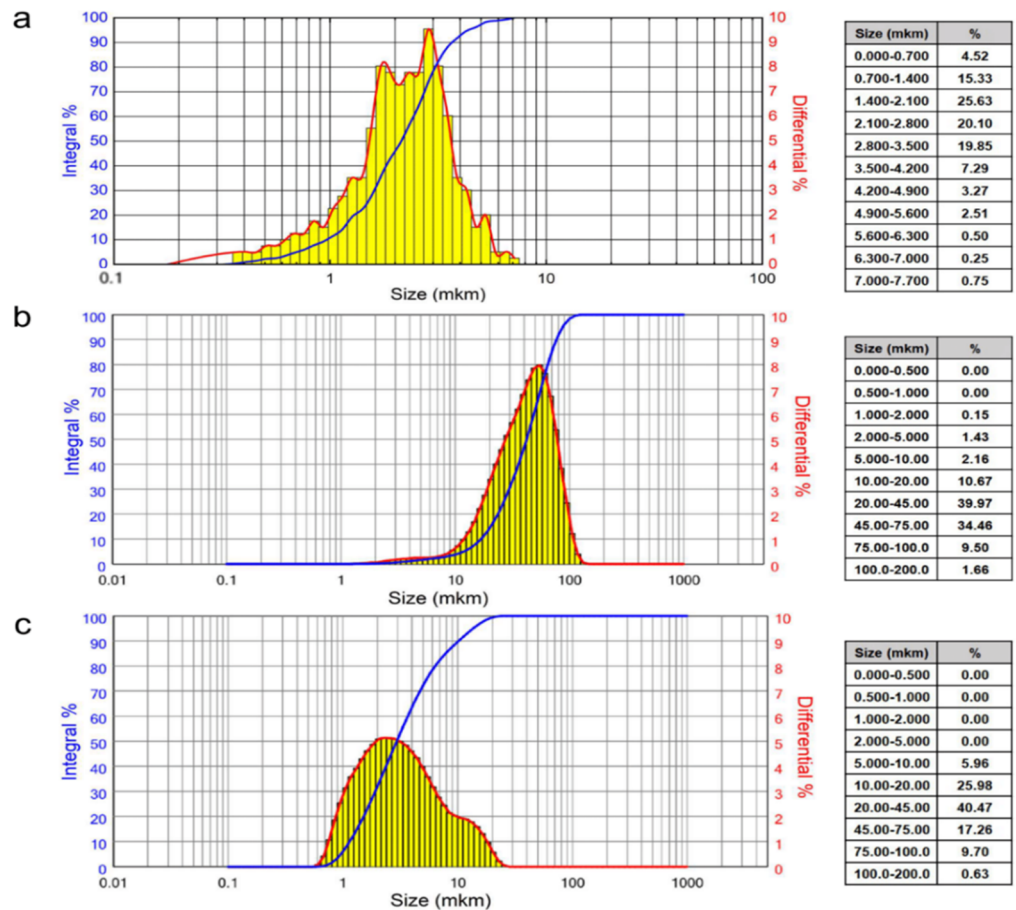


Figure 4. Particle size distribution histograms for antimicrobial additives: CuSO₄ powder (a); CuO powder (b); CuO microspheres (c).

The morphology of the additives' particles was studied using SEM. Figure 5 shows microphotographs of the general appearance of the antimicrobial additives' particles. It was found that the sample of commercial copper (II) sulphate was characterized by particles with a lamellar structure, which may be due to the formation of crystalline hydrates during sorption of water vapor from the atmosphere (Figure 5a,b). The CuSO₄ particles had a high specific surface area with a high variability in size and shape. The commercial CuO powder was characterized by coarsely dispersed irregularly shaped particles with numerous pores, and also had a large specific surface area (Figure 5c,d). On the contrary, CuO microspheres powder consisted of discrete particles, the shape of which was close to spherical (Figure 5e,f).

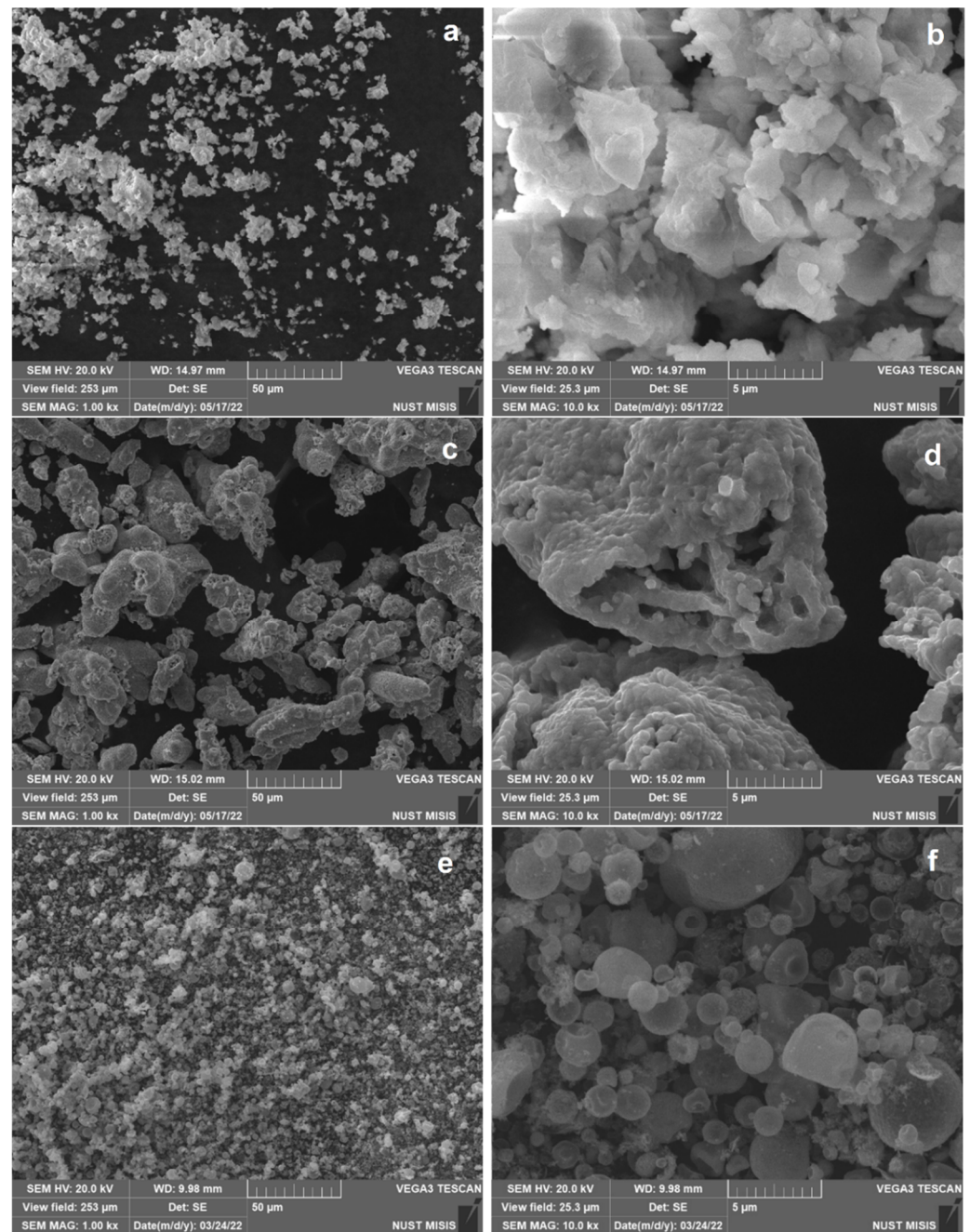


Figure 5. SEM micrographs of antimicrobial additive particles: CuSO_4 powder (a,b); CuO powder (c,d); CuO microspheres (e,f).

The true density of antimicrobial additives under study was analyzed by helium pycnometry. The density of CuSO_4 powder was 2.3 g/cm^3 , CuO powder— 6.4 g/cm^3 , and CuO microsphere powder— 6.1 g/cm^3 . The density decrease for copper (II) oxide microspheres is associated with internal porosity of the particles.

In order to characterize the volume parameters of CuO microsphere particles, the chipping structure of the particles was studied (Figure 6). The microspheres' particles were hollow spheres with a wall thickness ranging from 0.23 to $0.54 \mu\text{m}$. The inner volume of the microspheres was presumably filled with air and pyrolytic gas residues. The formation of a thin wall occurred during the process of mass transfer during pyrolysis. The particles with a size smaller than 100 nm were detected, which can explain the widening of maxima on the X-ray pattern of the sample. The presence of individual irregularly shaped particles

in the sample can be explained by differences in size of aerosol droplets and fluctuations in the concentration of the initial solution.

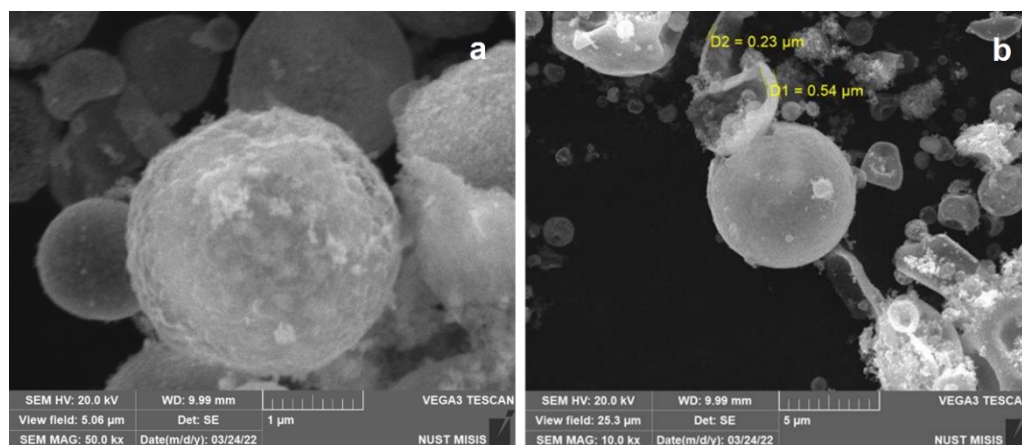


Figure 6. Structure analysis of CuO microspheres (SEM): general view of the microsphere (a), view of microsphere cleavage with measurement parameters (b).

4.2. Structure and Mechanical Properties of Composites

The structure of the sheet materials based on PLA with various additives was analyzed using SEM. The particle distribution character and the composites' structures are shown in Figure 7. The CuSO_4 particles tended to agglomerate in the PLA matrix (Figure 7a,b), which adversely affected the composite properties.

It was found that the PCL component formed rounded domains in the PLA matrix (Figure 7d), and it was not concentrated at the interface between copper (II) sulphate and PLA. So, it worked more like a PLA modifier rather than a PLA/particle compatibilizer providing a plasticizing effect on the rigid PLA matrix.

The copper (II) oxide powder created large agglomerates in the polymer matrix that could be visible in the material even to the naked eye (Figure 7e,f). In this case, the PLA matrix was characterized by a layered defective structure, which affected the embrittlement of the material.

The composites with hollow microspheres of CuO had a homogeneous structure of the matrix itself (Figure 7g,h). However, the microspheres destroyed during the manufacture of composites were found in a number of areas of analysis. To reduce the proportion of destroyed microspheres, it is advisable to reduce the intensity of shear loads when compounding the additive with the polymer.

Limiting the concentration of dispersed fillers is based on the decrease in strength and impact properties of materials at concentrations exceeding the specified upper threshold values. If the concentration of filler or additive exceeds the threshold values, an agglomeration of particles occurs in the polymer melt, and it leads to a decrease in strength characteristics [37].

The results of the study of stress–strain properties are presented in Table 3. The neat PLA is a rigid-chain and brittle polymer with a high strength (59.1 MPa) to be classified as a structural plastic. As a rule, the introduction of dispersed particles of additives into PLA leads to its embrittlement. In numerous studies, either plasticizing components have been used in a combination with dispersed additives [38], or elastic fillers [39].

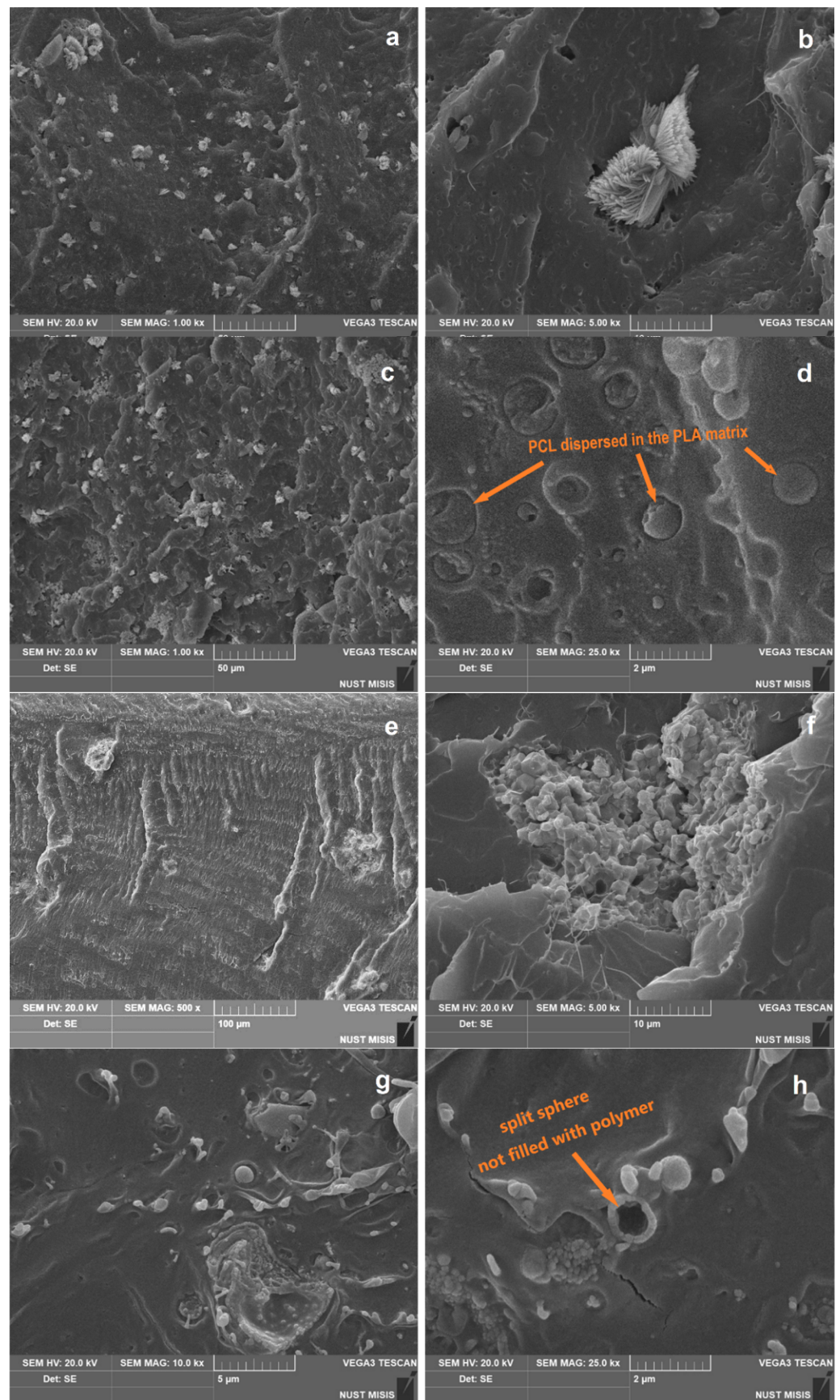


Figure 7. Morphology of cleavage of PLA-based composite: containing 10 wt.% CuSO_4 powder (a,b); containing 10 wt.% CuSO_4 and 5 wt.% PCL (c,d); containing 5 wt.% CuO powder (e,f); containing 5 wt.% CuO microspheres (g,h).

Table 3. Stress–strain properties of neat PLA and PLA-based composites.

Sample	σ_{max} * (MPa)	SD ** (MPa)/VaR *** (MPa ²)	ϵ_b **** (%)	SD (%)/VaR (%)	E ***** (GPa)	SD (GPa)/VaR (GPa ²)
PLA (neat)	59.1	2.8/7.7	5.8	0.6/0.4	3.67	0.09/0.01
PEG + 5 CuSO ₄	38.3	2.7/7.4	3.5	0.5/0.2	3.01	0.28/0.08
PEG + 10 CuSO ₄	27.3	1.8/3.4	6.0	0.8/4.4	2.98	0.18/0.03
PEG + PCL + 10 CuSO ₄	22.4	1.6/2.7	4.4	1.3/1.4	2.59	0.14/0.02
0.5 CuO	52.3	1.8/3.2	4.8	0.37/0.2	3.45	0.13/0.02
1 CuO	55.7	2.3/5.4	3.8	0.56/0.2	3.77	0.30/0.09
2 CuO	49.6	2.3/5.4	2.9	0.20/0.1	3.59	0.24/0.06
5 CuO	50.5	2.9/8.2	2.5	0.12/0.1	1.59	0.29/0.09
0.5 CuO sph	58.8	1.4/2.1	5.6	0.32/0.1	3.58	0.17/0.03
1 CuO sph	59.8	2.1/4.6	5.8	0.27/0.1	3.55	0.15/0.03
2 CuO sph	55.0	2.4/5.8	4.5	0.36/0.2	3.52	0.40/0.16
5 CuO sph	46.5	2.2/5.1	2.8	0.42/0.1	2.00	0.18/0.03

* σ_{max} —average ultimate tensile strength (arithmetic mean). ** SD—standard deviation. *** VaR—variance. **** ϵ_b —average relative elongation at break (arithmetic mean). ***** E—average modulus of elasticity (or Young's modulus) (arithmetic mean).

However, it is known that a low content of a dispersed additive (up to 5–10 wt.%) could improve the mechanical properties of PLA. This phenomenon is attributed to the uniform distribution of additive's particles [40]. According to the obtained results, adding 5–10 wt.% of the copper (II) sulphate to PLA induced a significant decrease in ultimate tensile strength (up to 55%) due to the agglomeration of particles in the polymer melt. Apparently, this was due to a high roughness of the additive's particles, which led to the formation of agglomerates larger than 10 μm . Thus, the limiting content of this additive in PLA was reduced.

Appending of the plasticizers as PCL and PEG in the composites led to a growth of relative elongation at break, while the modulus of elasticity decreased compared to the composites without plasticizer. The change of these parameters was associated with a decrease in the size of agglomerates of additive particles due to a good affinity of dispersed particles by low-molecular weight PEG or flexible-chain PCL [41].

The copper (II) oxide less effected the tensile strength and modulus of elasticity of the PLA matrix. The tensile modulus for PLA with additives of CuO powder and microspheres is comparable to that of neat PLA with an additive content of 0.5–2 wt.%. A sharp decrease in the elastic modulus (from 3.55 ± 0.05 GPa to 2.80 ± 0.20 GPa) was observed when going from 2 to 5 wt.% for both copper (II) oxide powder and microspheres. Thus, the additive content of 2 wt.% was a limit of the studied concentrations, a further increase in content contributed to a significant deterioration in properties.

It is important to note that the appending of CuO microspheres up to 1 wt.% led to a slight decrease in relative elongation and tensile strength, as well as in elastic modulus. This indicates a uniform distribution of the particles and a lack of structural defects during the fabrication of such composites [26]. A further increase in concentration of CuO microspheres led to a decrease in the ultimate strength by 9 ± 1 MPa compared to the neat PLA. This fact is explained by the achievement of the limiting concentration of the additive, at which it prevents the polymer matrix from bearing the load.

Compared to the CuO microspheres, the CuO powder significantly reduced the tensile strength parameter even at a content of 0.5 wt.%, which also proves the formation of large particle agglomerates as a result of their rough surface.

According to the analysis of the deformation-strength properties, it is possible to recommend the composites based on PLA containing PCL—10 wt.%, PEG—5 wt.%, CuSO₄—5 wt.%, and CuO powder or CuO microspheres—0.5–1 wt.% as more promising. At the same time, a combination of nano-dispersed particles of CuO with micro-sized CuSO₄ could provide an additional reinforcing effect.

Table 4 demonstrates the results of measuring density by the hydrostatic weighing method. The density of PLA increased slightly with the addition of all copper-containing particles. At the same time, the density of composites with both CuO powder and CuO microspheres practically did not differ, which might be due to the different nature of the distribution of additive particles in the matrix.

Table 4. Density of the PLA and PLA-based composites (hydrostatic weighing).

Sample	ρ^* (g/cm ³ , $\Delta \pm 0.002$ g/cm ³)	SD ** (g/cm ³)	VaR *** ((g/cm ³) ²)
PLA (neat)	1.248	0.011	0.0001
PEG + 5 CuSO ₄	1.276	0.009	0.0001
PEG + 10 CuSO ₄	1.329	0.008	0.0001
PEG + PCL + 10 CuSO ₄	1.317	0.007	0.0001
0.5 CuO	1.257	0.003	0.0001
1 CuO	1.255	0.004	0.0001
2 CuO	1.259	0.035	0.0001
5 CuO	1.293	0.016	0.0001
0.5 CuO sph	1.261	0.007	0.0001
1 CuO sph	1.263	0.002	0.0001
2 CuO sph	1.258	0.014	0.0001
5 CuO sph	1.273	0.022	0.0001

* ρ —average density (or specific gravity). ** SD—standard deviation. *** VaR—variance.

The influence of the studied copper-containing additives on mechanical properties of PLA illustrate the role of micro-sized particles in the formation of supramolecular structure of the composites. Table 5 demonstrates the thermophysical properties of PLA as a sole polymer and in the fabricated composites.

Table 5. Thermophysical properties of neat PLA and PLA as a component of the obtained composites (first heating).

Sample	Glass Transition			Cold Crystallization			Melting			
	T * (°C)	SD ***	T * (°C)	SD	ΔH ** (J/g)	SD	T * (°C)	SD	ΔH ** (J/g)	SD
PLA (neat)	58.7	0.4	-	-	-	-	148.7	0.6	13	2.5
PEG + 5 CuSO ₄	48.9	0.7	83.5	0.6	31	2.1	142.7/129.4	1.0	29	2.6
PEG + 10 CuSO ₄	50.1	0.8	89.5	0.9	34	3.3	147.8/135.7	0.8	27	2.4
PEG + PCL + 10 CuSO ₄	59.1	0.7	88.6	1.0	25	2.5	136.5/148.5	1.1	27	2.0
0.5 CuO	57.5	0.5	101.5	0.7	33	1.4	143.2/150.4	0.4	30	1.8
1 CuO	58.4	0.7	103.7	0.9	29	2.0	143.2/149.6	0.7	26	1.6
2 CuO	59.0	0.6	114.1	1.1	30	2.6	146.9/149.5	0.6	30	1.9
5 CuO	58.6	0.9	106.7	0.8	32	2.3	143.6/149.1	0.9	28	2.1
0.5 CuO sph	59.0	0.3	106.3	0.7	24	2.8	145.0/148.6	0.8	22	2.0
1 CuO sph	57.5	0.5	102.6	0.6	25	1.2	143.2/150.3	0.6	26	1.8
2 CuO sph	58.4	0.4	103.5	1.1	33	1.7	143.1/151.0	0.5	30	2.1
5 CuO sph	59.1	0.5	-	-	-	-	145.0/151.0	0.9	24	2.7

* T—average maximum temperature (arithmetic mean). ** ΔH —average enthalpy change (arithmetic mean). *** SD—standard deviation.

It was shown that CuO powder and CuO microspheres, along with their antimicrobial action, acted as crystallization nucleators for PLA to create a fine-crystalline structure with improved physical–mechanical properties.

According to the DSC results, the neat PLA was characterized by a glass transition temperature of 58.7 ± 0.5 °C and a melting temperature of 148.7 ± 0.5 °C. A peak of cold crystallization was small and diffuse, which indicated preferential crystallization of PLA

melt during cooling [42]. The particles of all the copper additives promoted recrystallization of PLA crystallites during heating, resulting in increasing the melting enthalpy for PLA crystallites. According to calculations, the enthalpy of crystallites melting increased from 13 J/g (for neat PLA) to 27–29 J/g (for PLA with CuSO₄), 26–28 J/g (for PLA with CuO), and 22–30 J/g (for PLA with CuO sph).

The thermograms showed a noticeable change in the shape (it became bimodal) of the PLA melting peak upon the presence of dispersed additives (Figure 8). The formation mechanism of double melting peaks is closely related to the cold crystallization behavior of PLA. It is known that the dispersed fillers can act as nucleating agents for heterogeneous crystallization of a polymer [43]. The bimodal peak indicated the formation of two populations of PLA crystallites: those formed during cooling of the bulk of the polymer, and those formed on the surface of additive particles after passing through the glass transition temperature of PLA (cold crystallization). Some imperfect crystals formed through the cold crystallization mechanism in the quick heating process. The population of these imperfect crystals melted at lower temperatures.

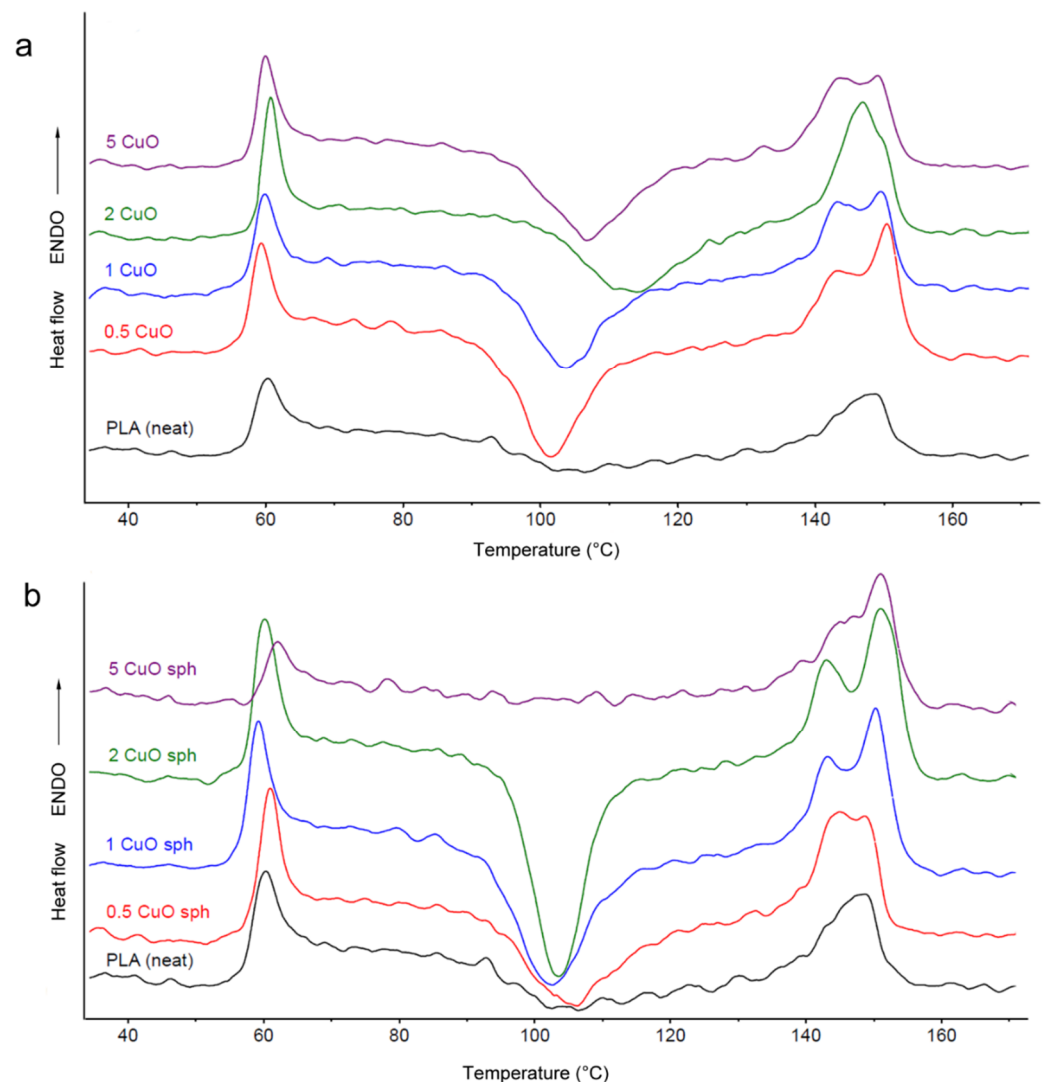


Figure 8. DCS curves of first heating of the neat PLA and PLA-based composites: containing 0.5–5 wt% CuO powder (a); 0.5–5 wt% CuO microspheres (b).

Moreover, there was a shift in the PLA melting peak to higher temperatures (by 1–2 °C), which indicated an increase in the perfection of crystalline grains. This phenomenon is known as a defect motion [44]. When passing through the glass transition temperature, the

mobility of PLA chains increases, which, in turn, facilitates the movement of defects inside crystalline formations, that is, the leveling of structural inhomogeneities occurs.

According to the DSC curves of the first melting of PLA composites with 2 and 5 wt.% CuO microspheres, in this concentration range, the limiting content of the additive was reached with the appearance of a percolation network of particles. This was also proven by the results of the stress–strain properties test. For the CuO powder, this saturation limit is apparently set at a higher content of additive due to a larger particle size.

5. Conclusions

In this study, a comparative analysis of the effect of copper (II) compounds in the form of dispersed particles and microspheres on the physical and mechanical properties of PLA-based composites was carried out. Together with traditional copper-based bactericidal fillers, hollow microspheres specially synthesized by spray pyrolysis were studied. In the presented work, composites with hollow microspheres were studied for the first time and their high manufacturability and ease of dispersion of microspheres in a PLA matrix were shown. The determined effect is associated with a regular spherical shape of the particles and the absence of aggregation. The analysis of morphological features of micro-sized particles and hollow microspheres made it possible to predict changes in the supramolecular organization of the polymer matrix and, as a response, the behavior of the polymer composite in the field of tensile forces.

It was found that the use of hollow microspheres, characterized by a reduced density and a regular spherical shape, leads to a significant improvement in the degree of dispersion in the volume of the polymer matrix during the formation of polymer composites in the field of high shear stresses (polymer processing). The microspheres and microparticles exhibit the properties of crystallization nuclei and contribute to the creation of a finely crystalline polymer structure with enhanced physical and mechanical characteristics. However, the agglomeration of powder additives during processing in a high-viscosity polymer melt leads to the opposite effect.

It was shown that the use of a plasticizer (PEG or PCL) creates conditions for high adhesion between particles of a hydrophilic additive and a hydrophobic polymer, which leads to a decrease in agglomeration of the additive and an increase in the physical–mechanical parameters of the polymer composite. At the same time, the possibility of creating hybrid polymer composites with increased antimicrobial properties based on a combination of micro-sized particles and microspheres based on copper-containing fillers in the PLA matrix is shown. The combination of “heavy” microparticles and “light” microspheres makes it possible to obtain materials with a uniform content of bactericidal copper compounds throughout the volume. Such composite materials are recommended for the production of medical device housings, sanitary equipment, and structural elements of public transport interiors. In the future, it is planned to study the biodegradability of the obtained materials, as well as to evaluate the antibacterial effectiveness of the proposed additives using biotesting techniques.

Author Contributions: Conceptualization, I.N.B. and A.A.O.; methodology, E.E.M. and B.B.K.; software, N.V.K.; validation, A.A.O. and E.E.M.; formal analysis, E.E.M.; investigation, N.V.V., T.B.K., E.E.M. and E.A.K.; resources, I.N.B. and E.E.M.; data curation, E.E.M.; writing—original draft preparation, I.N.B. and E.E.M.; writing—review and editing, E.E.M., N.V.K. and A.A.O.; visualization, N.V.K. and E.A.K.; supervision, I.N.B. and A.A.O.; project administration, I.N.B.; funding acquisition, I.N.B. and E.E.M. All authors have read and agreed to the published version of the manuscript.

Funding: E.E. Mastalygina is grateful for financial support to the Grant of the President of the Russian Federation (№ MK-3573.2022.1.3).

Acknowledgments: The authors express an acknowledgement to Joint Research Centre at Plekhanov Russian University of Economics for the access to the scientific equipment.

Conflicts of Interest: The authors declare no conflict of interest.

References

1. Scaffaro, R.; Botta, L.; Maio, A.; Gallo, G. Incorporation of an Antibiotic in Poly(Lactic Acid) and Polypropylene by Melt Processing. *J. Appl. Biomater. Funct. Mater.* **2016**, *14*, e240–e247. [[CrossRef](#)] [[PubMed](#)]
2. Ruh, E.; Mammadov, E. Antibacterial Activity of Ciprofloxacin-Impregnated 3D-Printed Polylactic Acid Discs: An in Vitro Study. *J. Infect. Dev. Ctries* **2022**, *16*, 484–490. [[CrossRef](#)] [[PubMed](#)]
3. Mahmoud Zaghoul, M.Y.; Yousry Zaghoul, M.M.; Yousry Zaghoul, M.M. Developments in Polyester Composite Materials—An in-Depth Review on Natural Fibres and Nano Fillers. *Compos. Struct.* **2021**, *278*, 114698. [[CrossRef](#)]
4. Macocinschi, D.; Filip, D.; Vlad, S.; Tuchilus, C.G.; Cristian, A.F.; Barboiu, M. Polyurethane/ β -Cyclodextrin/Ciprofloxacin Composite Films for Possible Medical Coatings with Antibacterial Properties. *J. Mater. Chem. B* **2014**, *2*, 681–690. [[CrossRef](#)] [[PubMed](#)]
5. Can Suner, S.; Yildirim, Y.; Yurt, F.; Ozel, D.; Oral, A.; Ozturk, I. Antibiotic Loaded Electrospun Poly (Lactic Acid) Nanofiber Mats for Drug Delivery System. *J. Drug Deliv. Sci. Technol.* **2022**, *71*, 103263. [[CrossRef](#)]
6. Youdhestar; Mahar, F.K.; Das, G.; Tajammul, A.; Ahmed, F.; Khatri, M.; Khan, S.; Khatri, Z. Fabrication of Ceftriaxone-Loaded Cellulose Acetate and Polyvinyl Alcohol Nanofibers and Their Antibacterial Evaluation. *Antibiotics* **2022**, *11*, 352. [[CrossRef](#)] [[PubMed](#)]
7. Khan, F.; Katara, R.; Ramteke, S. Enhancement of Bioavailability of Cefpodoxime Proxetil Using Different Polymeric Microparticles. *AAPS PharmSciTech* **2010**, *11*, 1368–1375. [[CrossRef](#)]
8. Bouarab-Chibane, L.; Forquet, V.; Lantéri, P.; Clément, Y.; Léonard-Akkari, L.; Oulahal, N.; Degraeve, P.; Bordes, C. Antibacterial Properties of Polyphenols: Characterization and QSAR (Quantitative Structure-Activity Relationship) Models. *Front. Microbiol.* **2019**, *10*, 829. [[CrossRef](#)]
9. Wen, Y.; Zhao, R.; Yin, X.; Shi, Y.; Fan, H.; Zhou, Y.; Tan, L. Antibacterial and Antioxidant Composite Fiber Prepared from Polyurethane and Polyacrylonitrile Containing Tea Polyphenols. *Fibers Polym.* **2020**, *21*, 103–110. [[CrossRef](#)]
10. Liu, S.; Qin, S.; He, M.; Zhou, D.; Qin, Q.; Wang, H. Current Applications of Poly(Lactic Acid) Composites in Tissue Engineering and Drug Delivery. *Compos. Part B Eng.* **2020**, *199*, 108238. [[CrossRef](#)]
11. Lemire, J.A.; Harrison, J.J.; Turner, R.J. Antimicrobial Activity of Metals: Mechanisms, Molecular Targets and Applications. *Nat. Rev. Microbiol.* **2013**, *11*, 371–384. [[CrossRef](#)] [[PubMed](#)]
12. Cioffi, N.; Torsi, L.; Ditaranto, N.; Tantillo, G.; Ghibelli, L.; Sabbatini, L.; Blevè-Zacheo, T.; D'Alessio, M.; Zambonin, P.G.; Traversa, E. Copper Nanoparticle/Polymer Composites with Antifungal and Bacteriostatic Properties. *Chem. Mater.* **2005**, *17*, 5255–5262. [[CrossRef](#)]
13. Hoque, J.; Yadav, V.; Prakash, R.G.; Sanyal, K.; Haldar, J. Dual-Function Polymer-Silver Nanocomposites for Rapid Killing of Microbes and Inhibiting Biofilms. *ACS Biomater. Sci. Eng.* **2019**, *5*, 81–91. [[CrossRef](#)] [[PubMed](#)]
14. Sato, M.; Kawata, A.; Morito, S.; Sato, Y.; Yamaguchi, I. Preparation and Properties of Polymer/Zinc Oxide Nanocomposites Using Functionalized Zinc Oxide Quantum Dots. *Eur. Polym. J.* **2008**, *44*, 3430–3438. [[CrossRef](#)]
15. Feng, S.; Zhang, F.; Ahmed, S.; Liu, Y. Physico-Mechanical and Antibacterial Properties of PLA/TiO₂ Composite Materials Synthesized via Electrospinning and Solution Casting Processes. *Coatings* **2019**, *9*, 525. [[CrossRef](#)]
16. Gurianov, Y.; Nakonechny, F.; Albo, Y.; Nisnevitch, M. Antibacterial Composites of Cuprous Oxide Nanoparticles and Polyethylene. *Int. J. Mol. Sci.* **2019**, *20*, 439. [[CrossRef](#)]
17. Olkhov, A.A.; Karpova, S.G.; Tubayeva, P.M.; Lobanov, A.V.; Kurnosov, A.S.; Mastalygina, E.E.; Iordanskii, A.L. Supramolecular Structure of Electrospun Ultrathin Fibers Based on Poly-(3-Hydroxybutyrate) with Zinc-Tetraphenylporphyrin Complex. *AIP Conf. Proc.* **2018**, *2051*, 020217. [[CrossRef](#)]
18. Zaghoul, M.M.Y.M. Mechanical Properties of Linear Low-Density Polyethylene Fire-Retarded with Melamine Polyphosphate. *J. Appl. Polym. Sci.* **2018**, *135*, 46770. [[CrossRef](#)]
19. Zaghoul, M.; Zaghoul, M.M.Y. Influence of Flame Retardant Magnesium Hydroxide on the Mechanical Properties of High Density Polyethylene Composites. *J. Reinf. Plast. Compos.* **2017**, *36*, 1802–1816. [[CrossRef](#)]
20. Zaghoul, M.M.Y.; Mohamed, Y.S.; El-Gamal, H. Fatigue and Tensile Behaviors of Fiber-Reinforced Thermosetting Composites Embedded with Nanoparticles. *J. Compos. Mater.* **2018**, *53*, 709–718. [[CrossRef](#)]
21. Sedlarik, V. Antimicrobial Modifications of Polymers. In *Biodegradation-Life of Science*; IntechOpen: London, UK, 2013; pp. 187–204. [[CrossRef](#)]
22. Cárdenas, G.; Díaz, V.J.; Meléndrez, M.F.; Cruzat, C.C.; García Cancino, A. Colloidal Cu Nanoparticles/Chitosan Composite Film Obtained by Microwave Heating for Food Package Applications. *Polym. Bull.* **2009**, *62*, 511–524. [[CrossRef](#)]
23. Palza, H. Antimicrobial Polymers with Metal Nanoparticles. *Int. J. Mol. Sci.* **2015**, *16*, 2099–2116. [[CrossRef](#)]
24. Llorens, A.; Lloret, E.; Picouet, P.A.; Trbojevič, R.; Fernandez, A. Metallic-Based Micro and Nanocomposites in Food Contact Materials and Active Food Packaging. *Trends Food Sci. Technol.* **2012**, *24*, 19–29. [[CrossRef](#)]
25. Gurianov, Y.; Nakonechny, F.; Albo, Y.; Nisnevitch, M. LLDPE Composites with Nanosized Copper and Copper Oxides for Water Disinfection. *Polymers* **2020**, *12*, 1713. [[CrossRef](#)] [[PubMed](#)]
26. Delgado, K.; Quijada, R.; Palma, R.; Palza, H. Polypropylene with Embedded Copper Metal or Copper Oxide Nanoparticles as a Novel Plastic Antimicrobial Agent. *Lett. Appl. Microbiol.* **2011**, *53*, 50–54. [[CrossRef](#)]
27. Bezza, F.A.; Tichapondwa, S.M.; Chirwa, E.M.N. Fabrication of Monodispersed Copper Oxide Nanoparticles with Potential Application as Antimicrobial Agents. *Sci. Rep.* **2020**, *10*, 16680. [[CrossRef](#)] [[PubMed](#)]

28. Chukhlanov, V.Y.; Selivanov, O.G.; Chukhlanova, N.V.; Mastalygina, E.E. Syntactic Foams for Filling Sealing Compositions Based on Epoxy Resin and Hollow Phenol-Formaldehyde Microspheres. *Polym. Sci. Ser. D* **2020**, *13*, 241–244. [[CrossRef](#)]
29. Zolkin, A.L.; Galanskiy, S.A.; Kuzmin, A.M. Perspectives for Use of Composite and Polymer Materials in Aircraft Construction. *IOP Conf. Ser. Mater. Sci. Eng.* **2021**, *1047*, 012023. [[CrossRef](#)]
30. Mastalygina, E.E.; Chukhlanov, V.Y. Dielectric Study of Syntactic Foams Based on Polydimethylsiloxane and Hollow Glass Microspheres at X-Band Microwave Frequency. *IOP Conf. Ser. Mater. Sci. Eng.* **2020**, *896*, 012101. [[CrossRef](#)]
31. Logutenko, O.A.; Titkov, A.I.; Vorobyov, A.M.; Lyakhov, N.Z. A Novel Method to Prepare Copper Microspheres via Chemical Reduction Route. *J. Mater. Res. Technol.* **2021**, *13*, 1254–1265. [[CrossRef](#)]
32. Zhu, H.; Wang, J.; Xu, G. Fast Synthesis of Cu₂O Hollow Microspheres and Their Application in DNA Biosensor of Hepatitis B Virus. *Cryst. Growth Des.* **2009**, *9*, 633–638. [[CrossRef](#)]
33. Chen, L.; Zhang, Y.; Zhu, P.; Zhou, F.; Zeng, W.; Lu, D.D.; Sun, R.; Wong, C. Copper Salts Mediated Morphological Transformation of Cu₂O from Cubes to Hierarchical Flower-like or Microspheres and Their Supercapacitors Performances. *Sci. Rep.* **2015**, *5*, 9672. [[CrossRef](#)] [[PubMed](#)]
34. Savioli Lopes, M.; Jardim, A.L.; Maciel Filho, R. Poly (Lactic Acid) Production for Tissue Engineering Applications. *Procedia Eng.* **2012**, *42*, 1402–1413. [[CrossRef](#)]
35. Yudin, A.; Shatrova, N.; Khaydarov, B.; Kuznetsov, D.; Dzidziguri, E.; Issi, J.P. Synthesis of Hollow Nanostructured Nickel Oxide Microspheres by Ultrasonic Spray Atomization. *J. Aerosol Sci.* **2016**, *98*, 30–40. [[CrossRef](#)]
36. Shelonkov, P.G.; Pantyukhov, P.V.; Popov, A.A. Highly Filled Biocomposites Based on Ethylene-Vinyl Acetate Copolymer and Wood Flour. *IOP Conf. Ser. Mater. Sci. Eng.* **2018**, *369*, 012043. [[CrossRef](#)]
37. Zare, Y. Study of Nanoparticles Aggregation/Agglomeration in Polymer Particulate Nanocomposites by Mechanical Properties. *Compos. Part A Appl. Sci. Manuf.* **2016**, *84*, 158–164. [[CrossRef](#)]
38. Sarasini, F.; Luzi, F.; Dominici, F.; Maffei, G.; Iannone, A.; Zuerro, A.; Lavecchia, R.; Torre, L.; Carbonell-Verdu, A.; Balart, R.; et al. Effect of Different Compatibilizers on Sustainable Composites Based on a PHBV/PBAT Matrix Filled with Coffee Silverskin. *Polymers* **2018**, *10*, 1256. [[CrossRef](#)]
39. Tertyshnaya, Y.V.; Karpova, S.G.; Podzorova, M.V.; Khvatov, A.V.; Moskovskiy, M.N. Thermal Properties and Dynamic Characteristics of Electrospun Polylactide/Natural Rubber Fibers during Disintegration in Soil. *Polymers* **2022**, *14*, 1058. [[CrossRef](#)]
40. Ho, M.P.; Lau, K.T.; Wang, H.; Hui, D. Improvement on the Properties of Polylactic Acid (PLA) Using Bamboo Charcoal Particles. *Compos. Part B Eng.* **2015**, *81*, 14–25. [[CrossRef](#)]
41. Rogovina, S.Z.; Aleksanyan, K.V.; Loginova, A.A.; Ivanushkina, N.E.; Vladimirov, L.V.; Prut, E.V.; Berlin, A.A. Influence of PEG on Mechanical Properties and Biodegradability of Composites Based on PLA and Starch. *Starch Stärke* **2018**, *70*, 1700268. [[CrossRef](#)]
42. Liu, Z.; Fu, M.; Ling, F.; Sui, G.; Bai, H.; Zhang, Q.; Fu, Q. Stereocomplex-Type Polylactide with Bimodal Melting Temperature Distribution: Toward Desirable Melt-Processability and Thermomechanical Performance. *Polymer* **2019**, *169*, 21–28. [[CrossRef](#)]
43. Liu, W.; Wu, X.; Chen, X.; Liu, S.; Zhang, C. Flexibly Controlling the Polycrystallinity and Improving the Foaming Behavior of Polylactic Acid via Three Strategies. *ACS Omega* **2022**, *7*, 6248–6260. [[CrossRef](#)]
44. Kubel, C.; Gonzalez-Ronda, L.; Drummy, L.F.; Martin, D.C. Defect-Mediated Curvature and Twisting in Polymer Crystals. *J. Phys. Org. Chem.* **2000**, *13*, 816–829. [[CrossRef](#)]